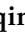


Brief Report

Crystal Structure of *Schizosaccharomyces pombe* Rho1 Reveals Its Evolutionary Relationship with Other Rho GTPases

Qingqing Huang ¹, Jiarong Xie ¹ and Jayaraman Seetharaman ^{2,*}

¹ Department of Biological Sciences, 14 Science Drive 4, National University of Singapore, Singapore 117543, Singapore

² Department of Structural Biology, St. Jude Children's Research Hospital, Memphis, TN 38105, USA

* Correspondence: seetharaman.jayaraman@stjude.org

Simple Summary: Rho family of proteins are involved in cytoskeletal organization, cell mobility and polarity, and are implicated in cancer morphogenesis. The structure and function of the Rho homologs from higher-level organisms are well studied, but not from the lower-level organisms. Such as over 95% of the known structures of Rho GTPases are from higher-order mammalian organisms, with only three structures of Rho homologs reported to date from lower-level, single-celled organisms. In this paper we report the crystal structure of Rho1 from *Schizosaccharomyces pombe*, also called fission yeast (*SpRho1*), in complex with GDP in the presence of Mg^{2+} at 2.63-Å resolution, to broaden our understanding of Rho homologs in lower-level organisms. Although the overall structure is similar to that of known Rho homologs, we observed subtle differences at the Switch I and II regions, in $\beta 2$ and $\beta 3$, and in the Rho insert domain and loop from Phe107 to Pro112. Combined with literature and sequence analyses, we suggest that the Switch regions and Rho insert domain may contribute to downstream kinase activation in different species through their interactions with different effectors and regulators; and the conservation and divergence of Rho GTPases among different species and provide evolutionary insight for *SpRho1*. While many studies have reported the evolutionary development of Rho GTPases based on their amino acid sequences, the present study, for the first time, explores these evolutionary aspects based on structure. Our analysis indicates that *SpRho1* is evolutionarily closer to *HsRhoC* than *HsRhoA*, as previously believed.



Citation: Huang, Q.; Xie, J.; Seetharaman, J. Crystal Structure of *Schizosaccharomyces pombe* Rho1 Reveals Its Evolutionary Relationship with Other Rho GTPases. *Biology* **2022**, *11*, 1627. <https://doi.org/10.3390/biology11111627>

Academic Editor: Scott Horowitz

Received: 26 September 2022

Accepted: 1 November 2022

Published: 7 November 2022

Publisher's Note: MDPI stays neutral with regard to jurisdictional claims in published maps and institutional affiliations.

Abstract: The Rho protein, a homolog of Ras, is a member of the Ras superfamily of small GTPases. Rho family proteins are involved in cytoskeletal organization, cell mobility, and polarity, and are implicated in cancer morphogenesis. Although Rho homologs from higher-order mammalian organisms are well studied, there are few studies examining Rho proteins in lower-level single-celled organisms. Here, we report on the crystal structure of Rho1 from *Schizosaccharomyces pombe* (*SpRho1*) in complex with GDP in the presence of Mg^{2+} at a 2.78 Å resolution. The overall structure is similar to that of known Rho homologs, including human RhoA, human RhoC, and *Aspergillus fumigatus* Rho1 (*AfRho1*), with some exceptions. We observed subtle differences at the Switch I and II regions, in $\beta 2$ and $\beta 3$, and in the Rho insert domain and loop from Phe107 to Pro112. Our analysis suggests that *SpRho1* is evolutionarily closer to *HsRhoC* than *HsRhoA*, as previously believed.

Keywords: GTPase; Rho; GDP; structure; evolution



Copyright: © 2022 by the authors. Licensee MDPI, Basel, Switzerland. This article is an open access article distributed under the terms and conditions of the Creative Commons Attribution (CC BY) license (<https://creativecommons.org/licenses/by/4.0/>).

1. Introduction

Hundreds of GTPases have been found in eukaryotic cells, playing various roles in signal transduction to control gene transcription, cell growth, and development. Small GTPases are a group of low-molecular-weight (20–25 kDa) guanine-nucleotide-binding proteins [1]. Most small GTPases comprise a conserved sequence of 5G boxes that are responsible for the GTPase activity and GTP/GDP binding [2]. Small GTPases can be divided into five families: Ras, Rho, Rab, Arf, and Ran. The Rho family was delineated

from the rest because of its unique insert region between the conserved G4 and G5 boxes, which is absent among other GTPase families. Like other Ras-like GTPases, Rho GTPases can switch between inactive GDP-bound and active GTP-bound forms through the actions of guanine nucleotide exchange factors (GEFs), GTPase-activating proteins (GAPs), and guanine nucleotide dissociation inhibitors (GDIs) [3]. GEFs are usually bound with inactive GDP-bound Rho and require the exchange of GDP with GTP for activation. The active GTP-Rho, subsequently, hydrolyzes GTP to GDP intrinsically, also in response to GAP stimulation. Finally, GDIs bind Rho to prohibit the actions of GEFs or GAPs to positively or negatively regulate Rho activity, respectively, as required within the cell [1,4,5].

The Rho family is divided into nine subfamilies, Rho, Rac, Cdc42, RhoDF, Rnd, RhoUV, RhoH, RhoBTB, and Miro, with various differences in sequence, structural motif, and function [1]. These Rho subfamily proteins are known to influence cell morphogenesis, mobility, adhesion, migration, and changes in polarity [6] by controlling the assembly, regulation, and reorganization of the actin cytoskeleton [7,8]. Different species have different isoforms of Rho family proteins, three of which are well studied in mammalian systems: RhoA, B, and C. Much less is known about Rho homologs from lower-level eukaryotes, such as yeast, which comprises a subfamily of five proteins: Rho1, -2, -3, -4, and -5.

Various structures of Rho GTPases have been reported on in complex with GDP/GTP analogs or effector proteins [9–13]. Over 95% of the known structures of Rho GTPases is from higher-order mammalian organisms, with only three structures of Rho homolog reported to date from lower-level, single-celled organisms. In this study, we report on the crystal structure of Rho1 from *Schizosaccharomyces pombe* (*SpRho1*), also called fission yeast, to broaden our understanding of Rho homologs in lower-level organisms. Sequence and structural analyses illustrate the conservation and divergence of Rho GTPases among different species and provide evolutionary insight for *SpRho1*. While many studies have reported on the evolutionary development of Rho GTPases based on their amino acid sequences, the present study, for the first time, explores these evolutionary aspects based on structure.

2. Results

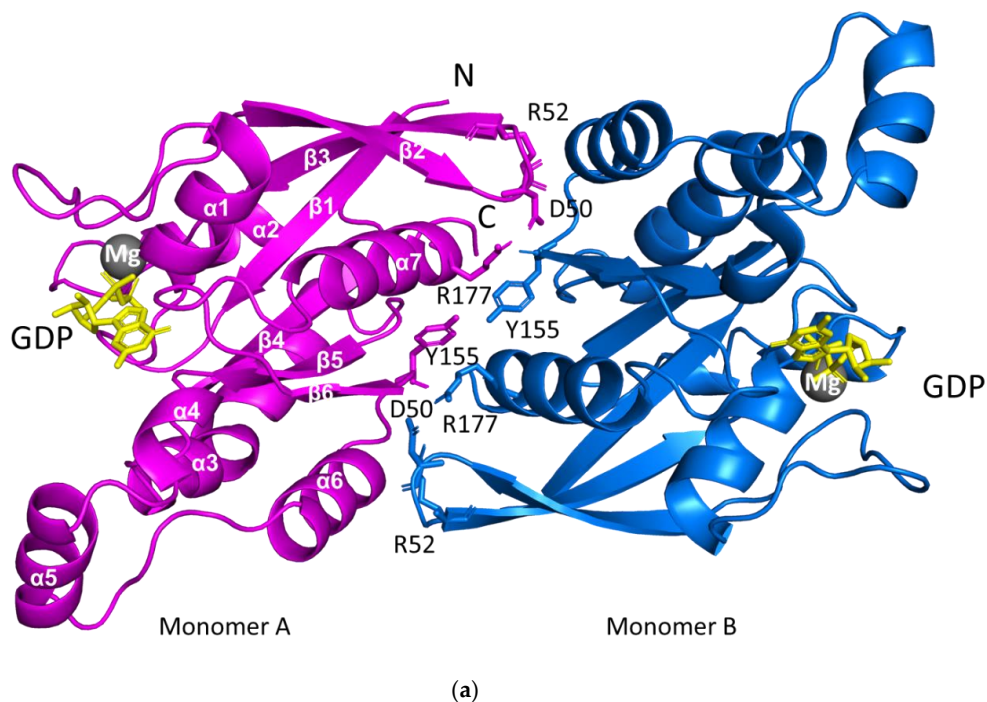
2.1. Structure of *SpRho1*–GDP Complex

The *SpRho1*–GDP complex structure was determined at a 2.78 Å resolution (Table 1). The gel filtration showed that the protein existed as a monomer, but the asymmetric unit comprised a dimeric *SpRho1*–GDP complex, which suggested the possibility of a monomer–dimer equilibrium in the solution. Monomers comprised of residues from Arg6 to Leu181 that were shown to be well defined in the electron density map. Each monomer of the dimer consisted of seven α -helices and a mixed twisted β -sheet consisting of six β -strands, of which five were parallel and one (the second) was antiparallel (Figure 1a). The *SpRho1* dimeric interface incorporated $\alpha 7$, the turn region between $\beta 2$ and $\beta 3$, with a total buried area of 1495 Å². The dimer was stabilized by several hydrogen-bonding contacts and hydrophobic interactions, with residues of Asp50, Arg52, Tyr155, and Arg177 from both monomers involved in hydrogen bonding (Table S1).

Table 1. Crystallographic data and refinement statistics for *Sp*Rho1–GDP complex with Mg²⁺.

Unit Cell Parameters (Å, °)	a = 105.69, b = 66.35, c = 75.55, α = γ = 90, β = 112.78
Space group	C2
Data collection	
Resolution range (Å)	50.00–2.78 (2.83–2.78) *
Wavelength (Å)	1.5418
Unique reflections	12485 (617)
Completeness (%)	100.0 (99.8)
Redundancy	4.4 (4.4)
Overall I/σ(I)	3.3 (2.8)
R _{sym} ^a	19.0 (0.818)
CC 1/2	0.952 (0.518)
CC *	0.988 (0.824)
Refinement and quality ^b	
Resolution range (Å)	50–2.78
R _{work} ^c	0.19
R _{free} ^d	0.23
Root mean square deviation	
Bond length (Å)	0.010
Bond angles (°)	1.466
Ramachandran statistics ^e	95.38
Favored (%)	
Outliers (%)	0.29 ^f
MolProbity score	2.00
Clashscore (all atoms)	6.48

* The high-resolution bin details are in the paratheses. ^a $R_{sym} = \sum |I_i - \langle I \rangle| / |I_i|$, where I_i is the intensity of the i^{th} measurement and $\langle I \rangle$ is the mean intensity for that reflection. ^b Reflections with $I > \sigma$ were used in the refinement. ^c $R_{work} = \sum |F_{obs} - F_{calc}| / |F_{obs}|$, where F_{calc} and F_{obs} are the calculated and observed structure amplitudes, respectively. ^d R_{free} is the same as R_{work} , but for 5–7% of the total, reflections were chosen at random and omitted from the refinement. ^e Ramachandran statistics were calculated using MolProbity (<http://molprobity.biochem.duke.edu/> accessed on 24 October 2022). ^f Residue Glu64 in chain B in a tight turn, whose side chain density was not well defined.

**Figure 1.** Cont.

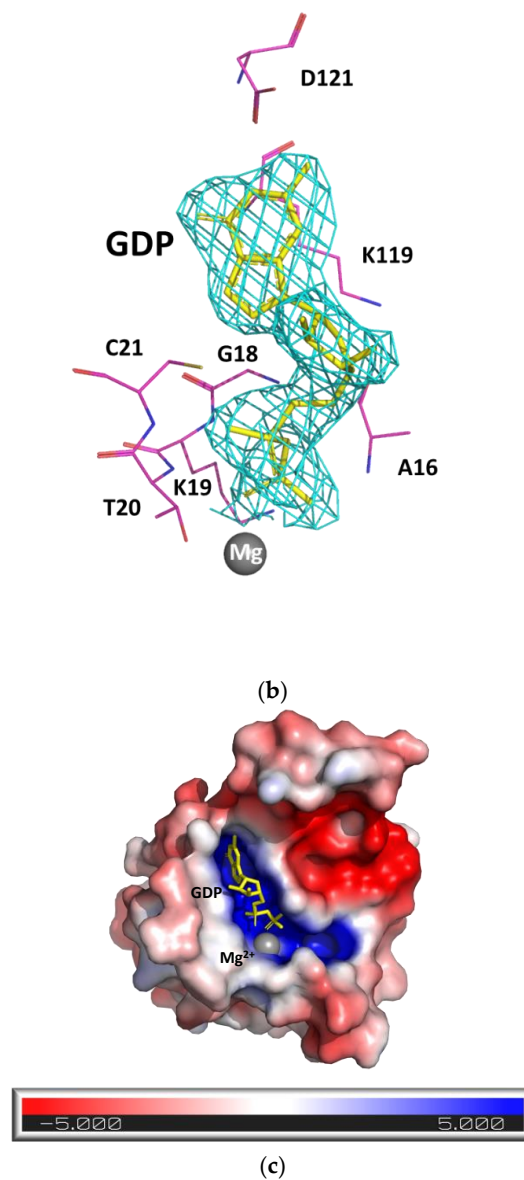


Figure 1. *SpRho1*–GDP–Mg²⁺ structure. (a) The ribbon diagram of the *SpRho1*–GDP–Mg²⁺ complex dimer. The GDP molecule is in yellow and Mg²⁺ is shown as a grey sphere. The key residues at the dimer interface are shown and labelled. The secondary structures are labelled on one monomer. (b) The $2F_o-F_c$ electron density around GDP with 1 sigma contour level. The key residues of the GDP binding pocket are shown. (c) Electrostatic surface potentials are colored red and blue for negative and positive charges, respectively, and white color represents neutral residues. The GDP is bound in the highly positively charged pocket. All the structurally related figures in this paper were prepared using PyMOL (The PyMOL Molecular Graphics System, Version 1.2r3pre, Schrödinger, LLC., New York, NY, USA).

2.2. Comparison of Rho Subfamily Protein Structures

Despite there being numerous structures of Rho subfamily proteins in the PDB database, only three Rho structures were reported on in complex with GDP and a Mg²⁺ ion (*HsRhoA*, *HsRhoC*, and *AfRho1*), with most structures shown in complex with effectors such as GDI or active GTP analogs, exhibiting conformational differences in the Switch I and II regions [9,14,15]. Since Mg²⁺ was known to affect the conformation of the Switch I region [16], we only compared our *SpRho1*–GDP–Mg²⁺ structure with the *HsRhoA*–GDP, *HsRhoC*–GDP, and *AfRho1*–GDP complexes also containing Mg²⁺ (Table S2).

We found that *SpRho1* resembled all three of the complexes examined, with good superimposition and RMSD values of less than 1 Å (Figure S1A). However, discrepancies were observed in five different regions (RMSD plot, Figure S1B), with subtle differences identified in the Switch I (Gly29–Ala45) and Switch II (Asp60–Val80) regions, the Rho insert domain, and at the loop region from Phe107 to Pro112. The fifth difference was observed only between *HsRhoA* and *SpRho1* in the β 2 and β 3 (Asn42–Asp60) region, with β 2 and β 3 of *HsRhoA* positioned further outward than that in *SpRho1*.

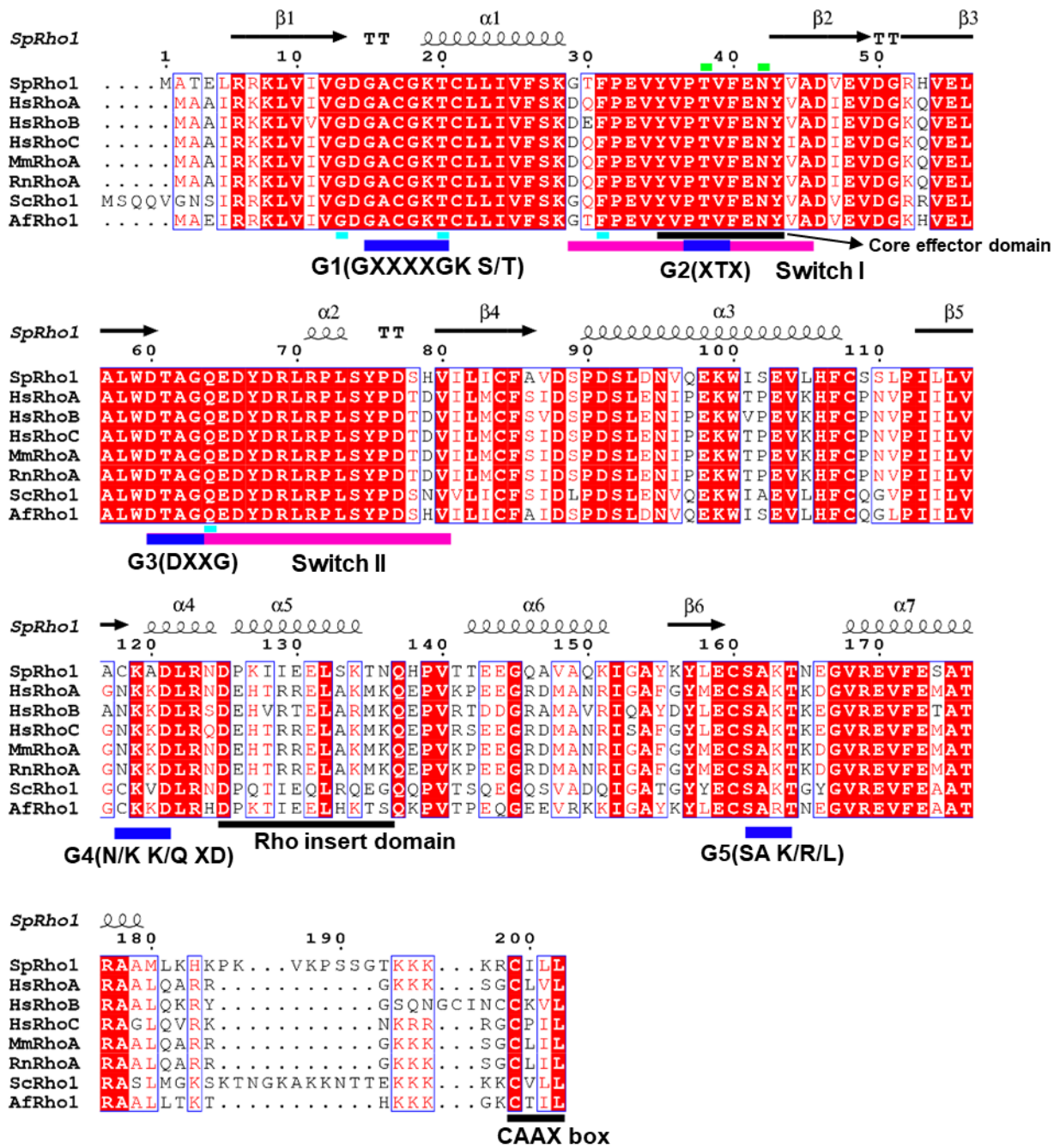
2.3. Sequence Comparison of Rho Subfamily Proteins

Rho family members share 30% identity with other Ras GTPases, and 40% to 80% sequence identity within the Rho family [1]. Sequence identity is even more conserved among the Rho subfamily members, with approximately 85% identity shared among *HsRhoA*, *HsRhoB*, and *HsRhoC* [8]. As would be expected, *SpRho1* shares a much greater sequence identity to homologs of lower-level organisms than mammalian organisms.

Sequence alignment showed several conserved regions between *SpRho1* and its homologs (Figure 2a). Specifically, the five G boxes are highly conserved and are involved in the exchange of GDP/GTP, GTP hydrolysis, and GTP-induced conformational change [2,8]. Wheeler and Ridley [17] identified the functional importance of Gly13, Thr20, Phe31, and Gln64 in the GTP hydrolysis of human Rho GTPases; we found that these residues were retained across all species, including yeast (Figure 2a). In addition, despite significant sequence conservation within the Switch I and Switch II regions, subtle conformational differences were observed for the inactive GDP-bound state (Figure S1A). These switches are turns between α -helices and β -strands, and serve as platforms for selective interactions with downstream factors to initiate cytoplasmic or nuclear signaling cascades [18,19]. Collectively, these observed structural differences may suggest different downstream activations among different species.

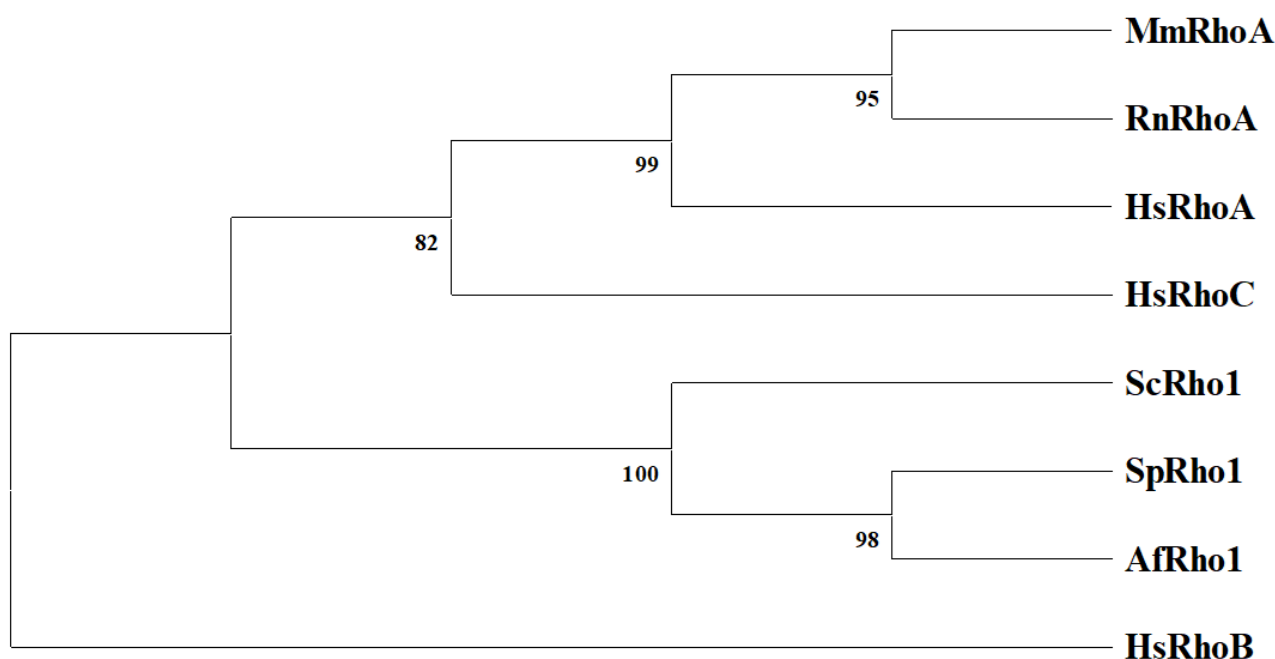
Apart from residues Asp125 and Leu132, the Rho insert domain (Asp125–Asn136) differs among species, with structural comparisons highlighting subtle differences within this region. The Rho insert domain is a signaling element found only in Rho family proteins, which reportedly has an impact on NADPH oxidase activation, Ras-induced apoptosis suppression, Rho kinase activation, and downstream cellular transformation [20–23].

Finally, there were clear differences between the yeast and mammalian proteins. The yeast Rho1 proteins (*SpRho1* and *ScRho1*) had 8 aa longer C-terminal tails (Pro185–Gly192) than their mammalian counterparts (Figure 2a), which may have a role in membrane localization [24]. Indeed, two signals are required for membrane localization: the CAAX box and a polybasic or polycysteine domain upstream of the prenylcysteine residue that is used for palmitoylation [23,24]. Additionally, compared with mammalian Rho GTPases, yeast Rho GTPases also have an abundance of hydrophilic amino acids, such as serine or threonine, and the presence of these residues may influence the differences in the localization patterns of mammalian and yeast Rho GTPases.



(a)

Figure 2. Cont.



(b)

Figure 2. Sequence alignment and phylogenetic tree of *SpRho1*. (a) Sequence alignment of *SpRho1*, HsRhoA, HsRhoB, HsRhoC, MmRhoA, RnRhoA, ScRho1, and AfRho1. These sequences were selected corresponding to Supplementary Table S2. The secondary structure of *SpRho1* is shown on the top. The blue bars represent the 5 conserved G boxes with specific sequences shown. The cyan bars (Gly13, Thr19, Phe30, and Gln63) indicate the important sites for GTP hydrolysis. Switch I and II regions are indicated with magenta bars. Core effector domain, Rho insert domain, and CAAX box are labelled with black bars. Blue frames indicate conserved residues. White letters in red boxes refer to strict identity, but red letters in white boxes indicate similarity. The amino acid sequences were aligned using Clustal Omega and Escript [25,26]. (b) Phylogenetic tree of *SpRho1*, HsRhoA, HsRhoB, HsRhoC, MmRhoA, RnRhoA, ScRho1, and AfRho1. It shows how species evolved from common ancestors and shows which are more related when they have a more recent common ancestor. The value at node indicates the frequency, which is the confidence of obtaining the same results using other programs. This reflects how species or other groups evolved from a series of common ancestors. Two species MEGA 11 software were used for preparing this tree [27].

2.4. Phylogenetic Analysis of Rho Subfamily Proteins

In exploring the evolutionary relationships between yeast and mammalian Rho proteins, we performed a phylogenetic tree analysis. We found a very early divergence of *HsRhoB* from the other Rho proteins, as well as a clustering of Rho1 proteins from lower-level, single-celled organisms, which may indicate a common ancestor (Figure 2b). Yeast *SpRho1* was evolutionarily closer to *AfRho1* than *ScRho1* from yeast *Saccharomyces cerevisiae*, because it shared a more recent common ancestor with *AfRho1*.

3. Discussion

Rho GTPases play essential roles in cellular development and signaling transduction. Previous structure/function analyses were primarily conducted using prototypical mammalian Rho GTPases, such as Rac1, RhoA, and Cdc42 [1,13,28,29]. Indeed, human RhoA is the most well-studied isoform from the Rho subfamily. RhoA shows extensive homology with other isoforms, such as RhoB or RhoC, with all three homologs playing similar functions in actin polymerization and stress fiber induction [17]. Numerous structures for human GDP/GTP-bound Rho proteins have been reported on, particularly RhoA in

complex with binding effectors (Table S2), albeit structural analyses for RhoB and RhoC are limited. The mouse Rho homolog has also been well studied compared to yeast and fungus homologs, whose investigations are highly limited. Thus, an understanding of the present structure of Rho1 from *S. pombe* is crucial in filling the gaps in our understanding of the evolutionary relationships of RhoA subfamily proteins from different species, particularly for lower-level organisms such as yeast and fungus.

Based on our structure–sequence relationships, we suggest that *SpRho1* may be evolutionarily closer to *HsRhoC* than to *HsRhoA*, as previously believed. Studies have shown that mammalian RhoA can substitute for *S. cerevisiae* Rho1 and confer full function in yeast cells [30]. The phylogenetic tree analysis, as predicted from amino acid sequences, indicated that *HsRhoA* and *HsRhoC* may have diverged at the same point from a Rho homolog from a single-celled organism (Figure 2a), suggesting a common ancestor for *HsRhoA*, *HsRhoC*, and *SpRho1*. As such, it is uncertain whether *HsRhoA* is evolutionarily closer than *HsRhoC*. The sequence analysis showed that *SpRho1* and *HsRhoC* had a 70% similarity, which was higher than that for *HsRhoA* with *SpRho1* (67%), albeit not significantly. Furthermore, the structure superimposition showed that 18 more C α atoms of *HsRhoC* could be superimposed to *SpRho1* compared with *HsRhoA*. These findings together may indicate that *HsRhoC* is evolutionarily closer to *SpRho1* than *HsRhoA* is. However, this assumption should be taken with caution as we could not exclude *HsRhoB* to be less related, because it branched off earlier in evolutionary history; indeed, *HsRhoB* shared a high sequence similarity with *SpRho1* (Figure 2b).

In conclusion, here, we determined and characterized the structure of *SpRho1* and highlighted its similarities with other reported Rho subfamily structures. Our analysis of the unique and conserved features of Rho homologs suggested that *SpRho1* is likely to be evolutionarily closer to *HsRhoC* than *HsRhoA*, and further predicted that the Rho insert region of the Rho GTPase likely contributes to the downstream kinase activation among different species; however, this warrants further studies. Our study offered further insight into the Rho protein family of single-celled organisms and the evolutionary conservation of this key protein compared with mammalian types, filling the gap in our understanding of the structure and function of RhoA proteins from lower-level organisms.

4. Methods and Materials

4.1. Protein Expression and Purification

BamHI and SalI sites were used for the cloning of the *Schizosaccharomyces pombe* Rho1 (*SpRho1*) gene (NCBI gene ID: 2541612) in the modified pET32b vector. The protein was fused with the N-terminal (His)₆ tag and expressed in the *Escherichia coli* BL21 strain. BL21 cells were cultured in LB broth medium with 100 μ g/mL ampicillin at 37 °C, and 150 μ M IPTG was added for induction. Cells were harvested with centrifugation at 3500 rpm (JLA-8.1 rotor) for 30 min at 4 °C. Cell pellets were lysed in a lysis buffer (50 mM Tris-HCl at pH7.4, 200 mM NaCl, 5% *v/v* glycerol, 5 mM imidazole, 0.1% *v/v* Triton x-100, a protease inhibitor, and 5 mM β -mercaptoethanol (BME)), and then sonicated. The lysate was then centrifuged and the supernatant was added to the Ni-NTA resin that was equilibrated with a lysis buffer for 1 hr at 4°C. Next, it was washed with a wash buffer (50 mM Tris-HCl (pH7.4), 200 mM NaCl, 5% *v/v* glycerol, 10 mM imidazole, and 5 mM 2-mercaptoethanol (BME)) twice, and then eluted with an elution buffer (the elution buffer contained 50 mM Tris-HCl (pH7.4), 200 mM NaCl, 5% *v/v* glycerol, 400 mM imidazole, and 5 mM 2-mercaptoethanol (BME)). The eluate was further purified using a Superdex 200 column (GE Healthcare, Uppsala, Sweden) with a buffer containing 20 mM Tris-HCl (pH7.4), 100 mM NaCl, 5% *v/v* glycerol, 5 mM MgCl₂, and 2 mM DTT. The purity was verified using 12.5% SDS-PAGE gel.

4.2. Crystallization and Structure Determination

The purified *SpRho1* was concentrated using 10 kDa MW cut-off centricon (vivaspin) to 6 mg/mL. GDP was added to the *SpRho1* protein to reach a molar ratio of 1:10 and

incubated for 5 min on ice. The complex was crystallized using the hanging drop vapor diffusion method at room temperature (24 °C) with commercial crystallization screening kits such as Crystal Screen 1 and 2, Salt Rx 1 and 2, and Index™ (Hampton Research), with a drop size 1:1 (μL) ratio of protein solution to reservoir solution. After the optimization of the initial conditions, diffraction quality crystals were obtained from a condition containing 0.2 M potassium sodium tartrate tetrahydrate, 0.1 M sodium citrate tribasic tetrahydrate (pH 5.6), and 1.9 M ammonium sulfate. Prior to data collection, the crystals were cryoprotected using the crystallization solution supplemented with 25% glycerol. The crystal diffracted up to 2.63 Å and data were collected using Rigaku MicroMax™-007 HF. The data were processed and scaled using HKL2000 [31]. There were two complex molecules in the asymmetric unit. PHENIX AUTO-MR [32] was used for structure determination using the PDB 1FTN as a search model for the molecular replacement method (Table S1). Model building was performed using COOT [33]. The final model had good stereochemical parameters, which were evaluated with PROCHECK [34].

Supplementary Materials: The following supporting information can be downloaded at: <https://www.mdpi.com/article/10.3390/biology11111627/s1>, Figure S1: Comparison of different Rho-GDP-Mg²⁺ structures. (A) Superimposition of SpRho1 (green) with HsRhoA (light blue, PDB code: 1FTN), HsRhoC (wheat, PDB code: 2GCN) and AfRho1 (cyan, PDB code: 5ZVP). The loop between F107 and P112, and the Rho insert domain from D125 to Q136 are highlighted with rectangles. Switch I region, Switch II region, β2, β3, the N and C termini are labeled. (B) The per-residue RMSD of the superimposed Rho-GDP-Mg²⁺ structures. The SpRho1 was set as a reference, for which the RMSD remains zero. Switch I, Switch II and Rho insert domain are shown with rectangles. β2 and β3 is indicated with straight line; Table S1: Hydrogen bonding contacts between the two monomers of the SpRho1 dimer; Table S2: Comparison between the SpRho1 and the other Rho subfamily proteins. References [10–12,15,35,36] are cited in the supplementary materials.

Author Contributions: Q.H.: formal analysis (equal); writing—Original draft (lead). J.X.: data curation (lead); methodology (equal). J.S.: conceptualization (lead); methodology (supporting); writing—Review and editing (lead). All authors have read and agreed to the published version of the manuscript.

Funding: This research received no external funding.

Institutional Review Board Statement: Not applicable.

Informed Consent Statement: Not applicable.

Data Availability Statement: The coordinates of the SpRho1 structure in the RCSB PDB database can be found under the code 8ETD.

Acknowledgments: The authors thank Vishnu Priyanka Reddy Chichili for her help with the crystallization.

Conflicts of Interest: The authors declare that they have no conflict of interest.

References

1. Beljan, S.; Bosnar, M.H.; Četković, H. Rho Family of Ras-Like GTPases in Early-Branching Animals. *Cells* **2020**, *9*, 2279. [CrossRef] [PubMed]
2. Bourne, H.R.; Sanders, D.A.; McCormick, F. The GTPase superfamily: Conserved structure and molecular mechanism. *Nature* **1991**, *349*, 117–127. [CrossRef] [PubMed]
3. Karnoub, A.E.; Symons, M.; Campbell, S.; Der, C.J. Molecular Basis for Rho GTPase Signaling Specificity. *Breast Cancer Res. Treat.* **2004**, *84*, 61–71. [CrossRef]
4. Longenecker, K.; Read, P.; Derewenda, U.; Dauter, Z.; Liu, X.; Garrard, S.; Walker, L.; Somlyo, A.V.; Nakamoto, R.K.; Somlyo, A.P.; et al. How RhoGDI binds Rho. *Acta Crystallogr. D Biol. Crystallogr.* **1999**, *55*, 1503–1515. [CrossRef] [PubMed]
5. Hakoshima, T.; Shimizu, T.; Maesaki, R. Structural Basis of the Rho GTPase Signaling. *J. Biochem.* **2003**, *134*, 327–331. [CrossRef] [PubMed]
6. Fort, P.; Blangy, A. The Evolutionary Landscape of Dbp-Like RhoGEF Families: Adapting Eukaryotic Cells to Environmental Signals. *Genome Biol. Evol.* **2017**, *9*, 1471–1486. [CrossRef]
7. Ridley, A.J.; Schwartz, M.A.; Burridge, K.; Firtel, R.A.; Ginsberg, M.H.; Borisy, G.; Parsons, J.T.; Horwitz, A.R. Cell Migration: Integrating Signals from Front to Back. *Science* **2003**, *302*, 1704–1709. [CrossRef]

8. Wennerberg, K.; Der, C.J. Rho-family GTPases: It's not only Rac and Rho (and I like it). *J. Cell Sci.* **2004**, *117*, 1301–1312. [[CrossRef](#)]
9. Ihara, K.; Muraguchi, S.; Kato, M.; Shimizu, T.; Shirakawa, M.; Kuroda, S.; Kaibuchi, K.; Hakoshima, T. Crystal Structure of Human RhoA in a Dominantly Active Form Complexed with a GTP Analogue. *J. Biol. Chem.* **1998**, *273*, 9656–9666. [[CrossRef](#)]
10. Bery, N.; Keller, L.; Soulié, M.; Gence, R.; Iscache, A.-L.; Cherier, J.; Cabantous, S.; Sordet, O.; Lajoie-Mazenc, I.; Pedelacq, J.-D.; et al. A Targeted Protein Degradation Cell-Based Screening for Nanobodies Selective toward the Cellular RHOB GTP-Bound Conformation. *Cell Chem. Biol.* **2019**, *26*, 1544–1558.e6. [[CrossRef](#)]
11. Trnimo, Z.; Guo, Z.; Gambin, Y.; Nguyen, U.T.T.; Wu, Y.; Abankwa, D.; Stigter, A.; Collins, B.; Waldmann, H.; Goody, R.; et al. Quantitative Analysis of Prenylated RhoA Interaction with Its Chaperone, RhoGDI. *J. Biol. Chem.* **2012**, *287*, 26549–26562. [[CrossRef](#)] [[PubMed](#)]
12. Jobichen, C.; Pal, K.; Swaminathan, K. Crystal structure of mouse RhoA:GTP γ S complex in a centered lattice. *J. Struct. Funct. Genom.* **2012**, *13*, 241–245. [[CrossRef](#)] [[PubMed](#)]
13. Wei, Y.; Zhang, Y.; Derewenda, U.; Liu, X.; Minor, W.; Nakamoto, R.K.; Somlyo, A.V.; Somlyo, A.P.; Derewenda, Z.S. Crystal structure of RhoA–GDP and its functional implications. *Nat. Struct. Mol. Biol.* **1997**, *4*, 699–703. [[CrossRef](#)] [[PubMed](#)]
14. Kristelly, R.; Gao, G.; Tesmer, J. Structural Determinants of RhoA Binding and Nucleotide Exchange in Leukemia-associated Rho Guanine-Nucleotide Exchange Factor. *J. Biol. Chem.* **2004**, *279*, 47352–47362. [[CrossRef](#)]
15. Dias, S.M.G.; Cerione, R.A. X-ray Crystal Structures Reveal Two Activated States for RhoC. *Biochemistry* **2007**, *46*, 6547–6558. [[CrossRef](#)]
16. Shimizu, T.; Ihara, K.; Maesaki, R.; Kuroda, S.; Kaibuchi, K.; Hakoshima, T. An Open Conformation of Switch I Revealed by the Crystal Structure of a Mg²⁺-free Form of RHOA Complexed with GDP. *J. Biol. Chem.* **2000**, *275*, 18311–18317. [[CrossRef](#)]
17. Wheeler, A.; Ridley, A. Why three Rho proteins? RhoA, RhoB, RhoC, and cell motility. *Exp. Cell Res.* **2004**, *301*, 43–49. [[CrossRef](#)]
18. Bishop, A.L.; Hall, A. Rho GTPases and their effector proteins. *Biochem. J.* **2000**, *348*, 241–255. [[CrossRef](#)]
19. Dvorský, R.; Ahmadian, M.R. Always look on the bright site of Rho: Structural implications for a conserved intermolecular interface. *EMBO Rep.* **2004**, *5*, 1130–1136. [[CrossRef](#)]
20. Nisimoto, Y.; Freeman, J.L.R.; Motalebi, S.A.; Hirshberg, M.; Lambeth, J.D. Rac Binding to p67. *J. Biol. Chem.* **1997**, *272*, 18834–18841. [[CrossRef](#)]
21. Karnoub, A.E.; Der, C.J.; Campbell, S.L. The Insert Region of Rac1 Is Essential for Membrane Ruffling but Not Cellular Transformation. *Mol. Cell. Biol.* **2001**, *21*, 2847–2857. [[CrossRef](#)] [[PubMed](#)]
22. Zong, H.; Kaibuchi, K.; Quilliam, L.A. The Insert Region of RhoA Is Essential for Rho Kinase Activation and Cellular Transformation. *Mol. Cell. Biol.* **2001**, *21*, 5287–5298. [[CrossRef](#)] [[PubMed](#)]
23. Hancock, J.P.; Paterson, H.; Marshall, J. A Polybasic Domain or Palmitoylation Is Required in Addition to the CAAX Motif to Localize ~21's to the Plasma Membrane. *Cell* **1990**, *63*, 133–139. [[CrossRef](#)]
24. Michaelson, D.; Silletti, J.; Murphy, G.; D'Eustachio, P.; Rush, M.; Philips, M.R. Differential Localization of Rho GTPases in Live Cells: Regulation by Hypervariable Regions and RhoGDI Binding. *J. Cell Biol.* **2001**, *152*, 16. [[CrossRef](#)] [[PubMed](#)]
25. Sievers, F.; Wilm, A.; Dineen, D.; Gibson, T.J.; Karplus, K.; Li, W.Z.; Lopez, R.; McWilliam, H.; Remmert, M.; Soding, J.; et al. Fast, scalable generation of high-quality protein multiple sequence alignments using Clustal Omega. *Mol. Syst. Biol.* **2011**, *7*, 539. [[CrossRef](#)]
26. Goujon, M.; McWilliam, H.; Li, W.Z.; Valentin, F.; Squizzato, S.; Paern, J.; Lopez, R. A new bioinformatics analysis tools framework at EMBL-EBI. *Nucleic Acids Res.* **2010**, *38*, W695–W699. [[CrossRef](#)]
27. Tamura, K.; Stecher, G.; Kumar, S. MEGA11: Molecular Evolutionary Genetics Analysis Version 11. *Mol. Biol. Evol.* **2021**, *7*, 3022–3027. [[CrossRef](#)]
28. Hirshberg, M.; Stockley, R.W.; Dodson, G.; Webb, M. The crystal structure of human rac1, a member of the rho-family complexed with a GTP analogue. *Nat. Struct. Mol. Biol.* **1997**, *4*, 147–152. [[CrossRef](#)]
29. Nassar, N.; Hoffman, G.R.; Manor, D.; Clardy, J.C.; Cerione, R.A. Structures of Cdc42 bound to the active and catalytically compromised forms of Cdc42GAP. *Nat. Struct. Mol. Biol.* **1998**, *5*, 1047–1052. [[CrossRef](#)]
30. Qadota, H.; Anraku, Y.; Botstein, D.; Ohya, Y. Conditional lethality of a yeast strain expressing human RHOA in place of RHO1. *Proc. Natl. Acad. Sci. USA* **1994**, *91*, 9317–9321. [[CrossRef](#)]
31. Otwinowski, Z.; Minor, W. Processing of X-ray diffraction data collected in oscillation mode. In *Methods in Enzymology*; Elsevier: Amsterdam, The Netherlands, 1997; Volume 276, pp. 307–326. Available online: <https://linkinghub.elsevier.com/retrieve/pii/S007668799776066X> (accessed on 4 May 2022).
32. Adams, P.D.; Afonine, P.V.; Bunkóczi, G.; Chen, V.B.; Davis, I.W.; Echols, N.; Headd, J.J.; Hung, L.-W.; Kapral, G.J.; Grosse-Kunstleve, R.W.; et al. PHENIX: A comprehensive Python-based system for macromolecular structure solution. *Acta Crystallogr. D Biol. Crystallogr.* **2010**, *66*, 213–221. [[CrossRef](#)] [[PubMed](#)]
33. Emsley, P.; Cowtan, K. Coot: Model-building tools for molecular graphics. *Acta Crystallogr. D Biol. Crystallogr.* **2004**, *D60*, 2126–2132. [[CrossRef](#)] [[PubMed](#)]
34. Laskowski, R.A.; MacArthur, M.W.; Moss, D.S.; Thornton, J.M. PROCHECK: A program to check the stereochemical quality of protein structures. *J. Appl. Crystallogr.* **1993**, *26*, 283–291. [[CrossRef](#)]
35. Rose, R.; Weyand, M.; Lammers, M.; Ishizaki, T.; Ahmadian, M.R.; Wittinghofer, A. Structural and mechanistic insights into the interaction between Rho and mammalian Dia. *Nature* **2005**, *435*, 513–518. [[CrossRef](#)] [[PubMed](#)]
36. Yamashita, M.; Kurokawa, K.; Sato, Y.; Yamagata, A.; Mimura, H.; Yoshikawa, A.; Sato, K.; Nakano, A.; Fukai, S. Structural basis for the Rho- and phosphoinositide-dependent localization of the exocyst subunit Sec3. *Nat. Struct. Mol. Biol.* **2010**, *17*, 180–186. [[CrossRef](#)] [[PubMed](#)]